Orientation selectivity based structure for texture classification

Wu, Jinjian; Lin, Weisi; Shi, Guangming; Zhang, Yazhong; Lu, Liu

2014

Wu, J., Lin, W., Shi, G., Zhang, Y., & Lu, L. (2014). Orientation selectivity based structure for texture classification. Proceedings of SPIE 9273, Optoelectronic Imaging and Multimedia Technology III, 9273.

https://hdl.handle.net/10356/106712

https://doi.org/10.1117/12.2071438

Orientation Selectivity based Structure for Texture Classification

Jinjian Wu[a], Weisi Lin[b], Guangming Shi[a], Yazhong Zhang[a], and Liu Lu [c]

[a]School of Electronic Engineering, Xidian University, Xi'an, China;
[b]School of Computer Engineering, Nanyang Technological University, Singapore;
[c]International Exchanges and Cooperation Centre, Xidian University, Xi'an, China

ABSTRACT

Local structure, e.g., local binary pattern (LBP), is widely used in texture classification. However, LBP is too sensitive to disturbance. In this paper, we introduce a novel structure for texture classification. Researches on cognitive neuroscience indicate that the primary visual cortex presents remarkable orientation selectivity for visual information extraction. Inspired by this, we investigate the orientation similarities among neighbor pixels, and propose an orientation selectivity based pattern for local structure description. Experimental results on texture classification demonstrate that the proposed structure descriptor is quite robust to disturbance.

Keywords: Texture Classification, Structure Descriptor, Orientation Selectivity Mechanism, Excitatory/Inhibitory Interaction

1. INTRODUCTION

The human visual system (HVS) is highly adaptive to extract structure from an image for scene perception and understanding.[1,2] Since structure represents the main visual information of an image, it is widely used in perception-oriented signal processing tasks, e.g., quality assessment,[3] image retrieval,[4] texture classification,[5] and so on.

Though local structure is used in a mass of image processing works, how to effectively extract structural information from an image is still an open problem. In the past decades, some local properties, such as the first order statistic values[2] (i.e., mean and variance), the luminance difference[6] (i.e., contrast and edge), and the quantity of information[7] (i.e. entropy), are chosen for image texture analysis. These descriptors are easy to implement and can effectively represent the intensity change of texture, but they cannot describe the spatial distribution of texture.[8] Considering the correlations among neighbor pixels, Ojala et al.[9] introduced a set of texture description models. According to the co-occurring pixel values in a local neighborhood, the spatial joint distribution is extracted for texture description. Moreover, the signed gray level difference is adopted to replace the absolute difference in the classical local binary pattern (LBP) texture descriptor,[5] with which the feature dimension is greatly decreased. Since the LBP is based on the signed gray level, it is too sensitive to small disturbance. However, the HVS is quite robust to disturbance when perceiving image content. Therefore, a more robust local structure descriptor, which can effectively describe the intensity change and spatial distribution, is demanded.

In this paper, we turn to investigate the property of HVS on structure perception and try to imitate the orientation selectivity mechanism for texture extraction. It is well known that the HVS is highly sensitive to the orientation information for image perception and understanding.[10] Moreover, neurophysiology research on visual cognition indicates that there are a kind of orientation selectivity neurons in the primary visual cortex.[11] According to the interactions among nearby neurons, they will tune specific orientations, which is called as orientation selectivity mechanism.[12,13] Furthermore, there exists two opponent interactions between these related neurons.[14] Generally speaking, neurons with similar preferred orientations tune to excitatory interactions, and neurons with opposite orientations tune to inhibitory interactions.[15] Therefore, the orientation selectivity mechanism in the primary visual cortex reveals the inner processing on image structure extraction.

E-mails: jinjian.wu@mail.xidian.edu.cn (J. Wu); wslin@ntu.edu.sg (W. Lin); gmshi@xidian.edu.cn (G. Shi)

Optoelectronic Imaging and Multimedia Technology III, edited by Qionghai Dai, Tsutomu Shimura,
Proc. of SPIE Vol. 9273, 92732M · © 2014 SPIE · CCC code: 0277-786X/14/$18
doi: 10.1117/12.2071438

By imitating the orientation selectivity mechanism, a novel local structure descriptor is introduced in this paper. Inspired by the orientation tuning in the primary visual cortex, the preferred orientation of each neuron is firstly estimated as the gradient direction of each pixel. Next, the spatial correlations among pixels are computed as the similarities of their preferred orientations. Meanwhile, the signed orientation similarity is employed to decide the excitatory/inhibitory interaction between two pixels. And then, the orientation selectivity based pattern of a pixel is computed as the arrangement of the singed values between a central pixel and its surrounding pixels. With the orientation selectivity based pattern, the spatial distribution of image texture can be effectively represented. Finally, by considering both of the intensity change and the orientation selectivity based pattern, a novel structure descriptor is created. The proposed structure descriptor is applied in texture classification. Experimental results on two large datasets demonstrate that the proposed model is rotation invariant, and it is much more robust to disturbance than the classic LBP[5,16] for texture classification.

The rest of this paper is organized as follows. In Section 2, the orientation selectivity mechanism is explored and an orientation selectivity based structure descriptor is introduced. The performance of the proposed structure descriptor on texture classification is demonstrated in section 3. Finally, we draw the conclusions in Section 4.

2. ORIENTATION SELECTIVITY BASED TEXTURE EXTRACTION

In this section, the orientation selectivity based pattern is firstly introduced to represent the spatial distribution of image texture. Next, by considering the orientation selectivity based pattern and the intensity change, a novel structure descriptor is created for texture extraction.

2.1 Orientation Selectivity based Pattern

Neuroscience researches indicate that the primary visual cortex presents substantial orientation selectivity when the human eye perceiving images.[12] During the past decades, the orientation selectivity mechanism has been throughly investigated.[17,18] Moreover, orientation selectivity has been one of the standard models to interpret how the HVS performs a complex computation for visual perception.[19,20] The origin of orientation selectivity is directly related to the spatial arrangement of intracortical responses in a local receptive field of the primary visual cortex.[12,21] Furthermore, the intracortical responses among neurons present two spatial opponent interaction, namely, excitatory and inhibitory interactions.[22] As shown in Fig. 1, cortical neurons with similar preferred orientations are more likely to present excitatory interactions ('+'), and these with different preferred orientations are more likely to present inhibitory interactions ('-').[19] The spatial arrangement of the excitatory and inhibitory neurons in a subfield displays the pattern of orientation selectivity.[21]

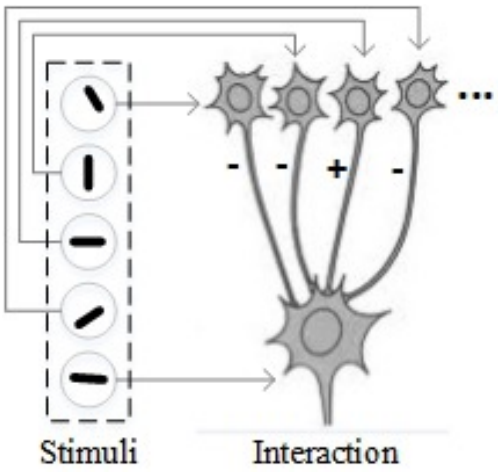

Figure 1: The interactions among cortical cells, where '+' means excitatory interaction and '-' means inhibitory interaction.

The orientation selectivity mechanism reveals the inner processing of structure extraction.[19] Thus, we try to design a novel structure descriptor by imitating the orientation selectively mechanism. The arrangement of the excitatory and inhibitory interactions in a local subfield can efficiently express the spatial correlation of structure.[12] Inspired by this, the spatial distribution of image structure can be computed as the organization of the preferred orientations among nearby pixels. For a given image $\mathcal{F}^{N\times N}$, the spatial distribution characteristic of structure for a pixel $x \in \mathcal{F}^{N\times N}$ can be expressed as the correlation between x and its neighborhood $\mathcal{X}=\{x_1, x_2, \cdots, x_n\}$,

$$\mathcal{P}(x|\mathcal{X}) = \mathcal{A}(\mathcal{I}(x|\mathcal{X})) = \mathcal{A}(\mathcal{I}(x|x_1, x_2, \cdots, x_n)), \tag{1}$$

where $\mathcal{P}(x|\mathcal{X})$ represents the spatial distribution of structure for pixel x, $\mathcal{A}(\cdot)$ represents the arrangement of responses, and $\mathcal{I}(x|\mathcal{X})$ represents the interaction between x and $\mathcal{X}$.

Since the cortical neurons in a local receptive field are connected with each other, pixels $x_i \in \mathcal{X}$ are not independent but correlated. In order to simplify the interactions between x and its neighborhood $\mathcal{X}=\{x_1, x_2, \cdots, x_n\}$, Hubel and Wiesel proposed to only consider the connections between two neurons in the feedforward model.[12,19] As a result, (1) can be reorganized as

$$\mathcal{P}(x|\mathcal{X}) \approx \mathcal{A}(\mathcal{I}(x|x_1), \mathcal{I}(x|x_2), \cdots, \mathcal{I}(x|x_n)), \tag{2}$$

where $\mathcal{I}(x|x_i)$ is the interaction between x and x_i.

As mentioned above, there exists two opponent interactions, namely, excitatory ('+') and inhibitory ('-') interactions. The interaction type between two cortical neurons is determined by the similarity of their preferred orientation. Researches on synaptic plasticity introduced a correlation-based rule for spatial interaction.[18,21] According to this rule, neurons with similar preferred orientations have a higher probability of connection and are more likely to respond as excitatory interactions. For example, as shown in Fig. 1, the third stimulus and the last stimulus have quite similar orientation, and they respond as excitatory interaction. While neurons with dissimilar preferred orientations are more likely to respond as inhibitory interactions. For example, as shown in Fig. 1, the first stimulus (also the second and the fourth stimuli) has quite different orientation with the last stimulus, and the interaction between them is inhibitory. Inspired by the feedforward model, we try to estimate the interaction type $\mathcal{I}(x|x_i)$ based on the preferred orientations between x and x_i.

Firstly, the preferred orientation θ of each pixel $x \in \mathcal{F}$ is computed as its gradient orientation,

$$\theta(x) = \arctan \frac{G_v(x)}{G_h(x)}, \tag{3}$$

where G_h and G_v are the gradient magnitudes alone the horizontal and vertical directions, respectively. In this paper, G_h and G_v are acquired with the Prewitt filters,

$$G_h = \mathcal{F} * f_h, \quad G_v = \mathcal{F} * f_v, \tag{4}$$

$$f_h = \frac{1}{3}\begin{bmatrix} 1 & 0 & -1 \\ 1 & 0 & -1 \\ 1 & 0 & -1 \end{bmatrix}, \; f_v = \frac{1}{3}\begin{bmatrix} 1 & 1 & 1 \\ 0 & 0 & 0 \\ -1 & -1 & -1 \end{bmatrix}, \tag{5}$$

where $*$ denotes the convolution operation.

Then, the interaction type $\mathcal{I}(x|x_i)$ between two pixels x and x_i is estimated with the similarity of their preferred orientations,

$$\mathcal{I}(x|x_i) = \begin{cases} 1 & \text{if } |\theta(x) - \theta(x_i)| < \mathcal{T} \\ 0 & \text{else} \end{cases}, \tag{6}$$

where '1' represents excitatory interaction, '0' represents inhibitory interaction, and $\mathcal{T}$ is the decision threshold. Researches on visual masking of human eye[23] demonstrates that nearby signals with same orientations cause strong masking effect, and the masking effect becomes weak when the differences among their orientations are larger than a certain threshold (e.g., 12°). Thus, we set $\mathcal{T}$=6° in this paper.

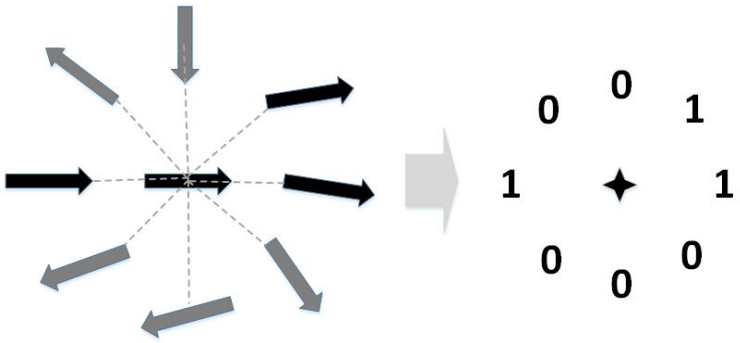

Figure 2: A example of orientation selectivity based pattern. Pixels which have similar preferred orientations to the central pixel respond as excitation ('1'), and these dissimilar ones respond as inhibition ('0').

Finally, by considering all of the interaction types between a central pixel and its surrounding pixels, an orientation selectivity based pattern is acquired, which is composed by a set of binary values and can effectively represent the spatial distribution of structure. In order to visualize how the orientation selectivity based pattern varies with the spatial orientation correlations, an example of the spatial arrangement of cortical stimuli and its corresponding interaction pattern are given in Fig. 2. By comparing the orientation of the central pixel and its 8-neighbor pixels (i.e., the size of the neighborhood $\mathcal{X}$ is set as n=8), As shown in Fig. 2, these neighbor pixels possess similar preferred orientations with the central one present excitatory interaction, and vice versa. As a result, the spatial correlation between the central pixel and its 8-neighbor surrounding is simplified into a 8-binary-value pattern.

There are too many types of orientation selectivity based pattern. For example, a 8-neighbor local region will present 2^8 different types of pattern. In order to reduce the pattern number, we explore the relationships among these patterns for further combination. During experiment we have found that these patterns with same excitatory subfield (where the excitatory interaction respond) are more correlated and represent much similar response. For example, as the second column shown in Fig. 3, the excitatory subfields (i.e., the sector domain that value '1' located) of the two patterns [00000001] and [00000010] are the same (within a 45° sector domain). As the last column shown in Fig. 3, the excitatory values of the two patterns [11111110] and 11111010 locate in a

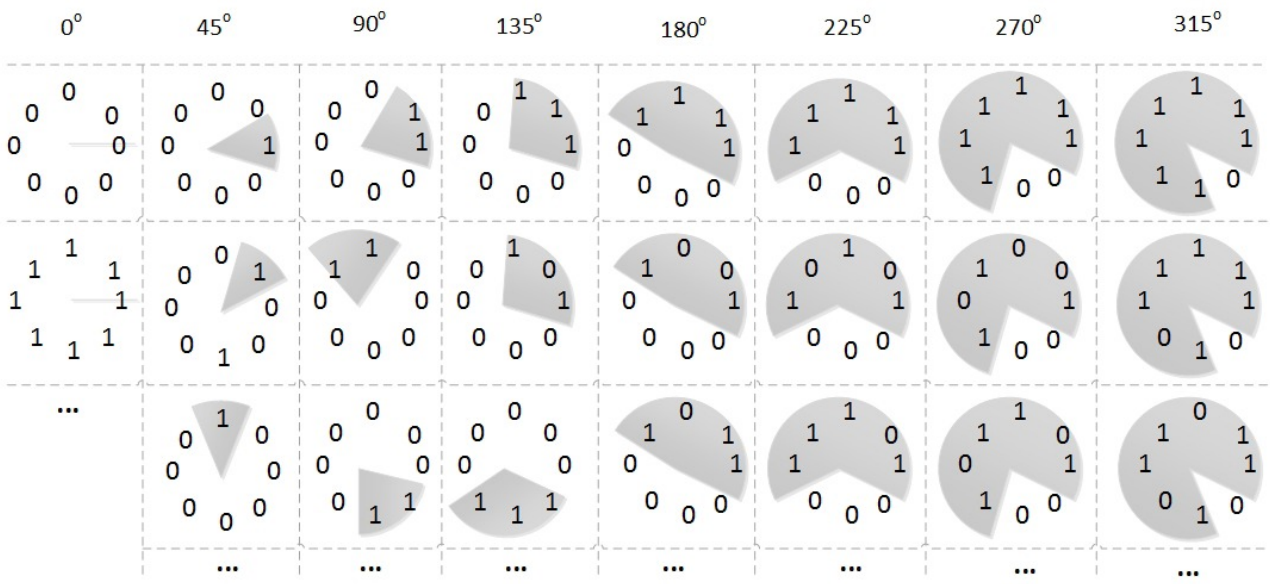

Figure 3: The combination of orientation selectivity based pattern based on their excitation subfield.

315° sector domain, and the two patterns present extremely similar spatial correlation. Therefore, we suggest to combine patterns according to their excitatory subfield. For example, for a 8-neighbor local region, all of the 256 patterns can be combined into 8 different kinds of sector domains, i.e., $\{0°, 45°, \cdots, 315°\}$, as shown in Fig. 3. As a result, the number of patterns is greatly decreased.

2.2 Texture Extraction

A successful structure descriptor should effectively represent the spatial correlation and intensity change of a local region. The spatial distribution of texture is analyzed with the orientation selectivity based pattern in the above subsection. Here, we compute the intensity change of a local region as its gradient magnitude,

$$\mathcal{M}(x) = \sqrt{(G_h(x))^2 + (G_v(x))^2}, \tag{7}$$

where $G_h(x)$ and $G_v(x)$ are the gradient magnitudes of pixel x alone the horizontal and vertical directions, respectively. The values of $G_h(x)$ and $G_v(x)$ can be acquired with (4).

By combining the orientation selectivity based pattern $\mathcal{P}$ and the gradient magnitude $\mathcal{M}$, a novel structure descriptor $\{\mathcal{P}/\mathcal{M}\}$ is created for texture extraction. Firstly, $\{\mathcal{P}/\mathcal{M}\}$ for each pixel is computed. Generally speaking, the texture characteristic of an image is represented by its textural histogram. Therefore, the $\{\mathcal{P}/\mathcal{M}\}$ values are mapped for constructing textural histogram.

There are two types of mapping methods: 1) directly calculate the number of orientation selectivity based patterns, which we called as *O*rientation *S*electivity based *T*extural (OST) histogram; 2) the contribution of gradient magnitude is considered, and the weighted distribution of orientation selectivity based patterns is calculated, which we called as *W*eighted *O*rientation *S*electivity based *T*extural (WOST) histogram. For the first type of mapping, the textural histogram is mapped as,

$$H(k) = \sum_{x=1}^{N} \delta(\mathcal{P}(x), \mathcal{P}^k), \tag{8}$$

$$\delta(\mathcal{P}(x), \mathcal{P}^k) = \begin{cases} 1 & \text{if } \mathcal{P}(x) = \mathcal{P}^k \\ 0 & \text{else} \end{cases}, \tag{9}$$

where N is the size of the image $\mathcal{I}$, and $\mathcal{P}^k$ is the $k{-}th$ orientation selectivity based pattern.

For the second type of mapping,the contribution of the gradient magnitude is considered, and the weighted textural histogram is mapped as,

$$H_w(k) = \sum_{x=1}^{N} w(x)\ \delta(\mathcal{P}(x), \mathcal{P}^k), \tag{10}$$

where $w(x)$ is the weight due to the gradient magnitude of pixel x, and we set $w(x){=}\mathcal{M}(x)$ for simplicity in this paper.

3. EXPERIMENTAL RESULTS

The proposed structure descriptor is quite consistent with the subjective perception. In order to demonstrate its effectiveness, we firstly illustrate its rotation invariance for texture description. Next, the robustness of the proposed structure descriptor on noise is demonstrated for texture classification.

The proposed structure descriptor is rotation invariance. Fig. 4 (a)-(c) show three textural images, which possess a same texton and different rotations (the rotation angles for Fig. 4 (a)-(c) are 0°, 45°, and 90°, respectively). Their corresponding OST based histograms are mapped with (8), as shown in Fig. 4 (d). As can be seen, the OST based histograms of Fig. 4 (a) and (c) (as the blue and red bars shown in Fig.fig:exam-ri (d)) are almost same. There are a little bit of difference between the OST based histograms of Fig. 4 (a) and (b). That is because with the rotation of the 45°, there exist a bit of difference in visual contents for the two image. In summary, the OST histograms for the three images are quite similar, which confirms that the proposed structure descriptor is rotation invariance.

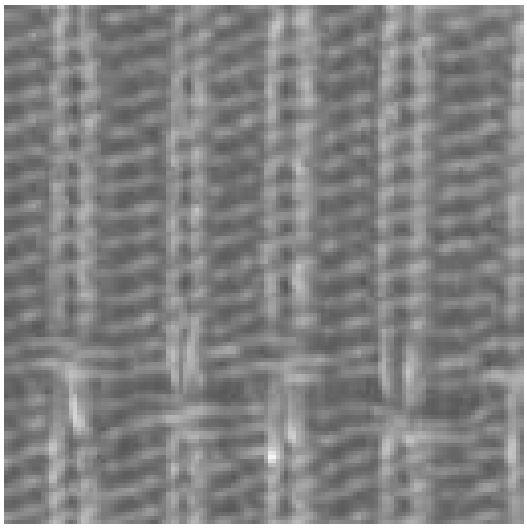

(a) 0°

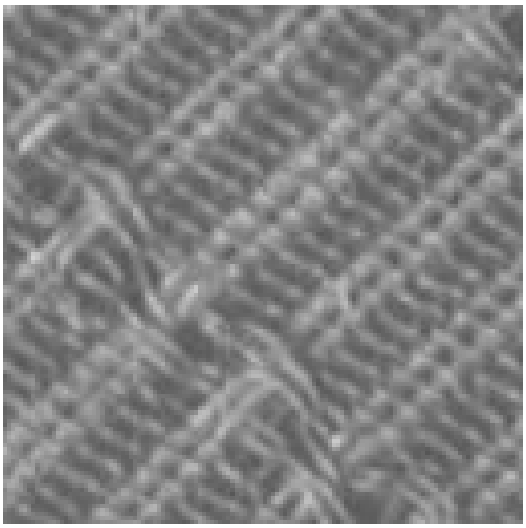

(b) 45°

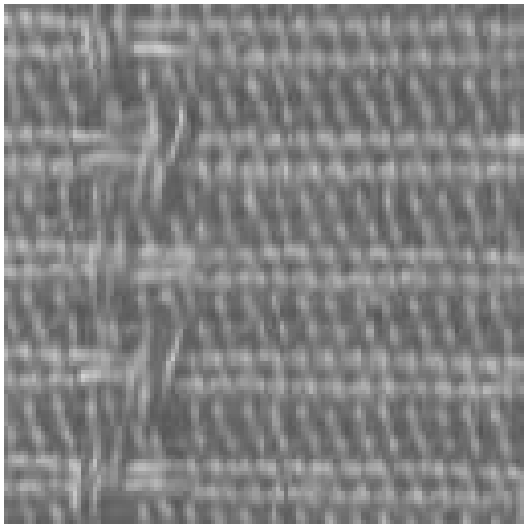

(c) 90°

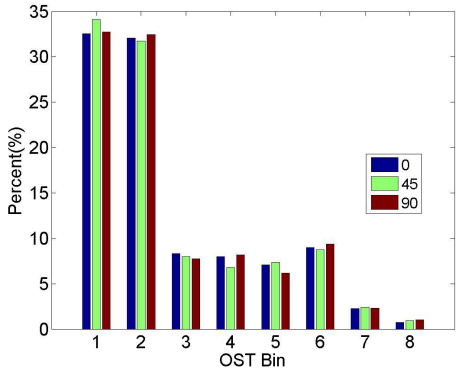

(d) OST based histogram

Figure 4: The OST based histograms for three texture images. The three texture images possess a same type of texton while under three different rotation angles.

The proposed structure descriptor is adopted for texture classification. Firstly, the image texture is extracted and mapped into histogram. Next, the chi-square distance is employed to calculated the difference between two textural histograms H_1 and H_2. The chi-square distance function is regarded as the weighted L^2-norm between two histograms,

$$D(H_1, H_2) = \sum_{k=1}^{n} \frac{(H_1(k) - H_2(k))^2}{H_1(k) + H_2(k)}. \tag{11}$$

In this paper, a publicly textural database, namely Outex,[24] is chosen for texture classification. Outex database includes 24 classes of textures, and each class of texture possess three illuminations ('horizon', 'inca', and 't184') and nine angles (0°, 5°, 10°, 15°, 30°, 45°, 60°, 75°, and 90°). The experiments are carried on two test suites of Outex database, namely, Outex_TC_00010 (TC10 for short) and Outex_TC_00012 (TC12 for short), which include the same 24 classes of textures. As in[16] described, the training/testing conditions for TC10 and TC12 are listed as follows,

- On TC10 suite: images under 'inca' illumination and '0°' angle (totally 480 images) are chosen for classifier training, and the other images for testing (480×8 images).
- On TC12 suite: the classifier is trained under the same training condition as that for TC10, and is tested on images under two (i.e., 't184' and 'horizon') illuminations and nine angles (480×2×9 images).

The performances of the proposed OST and WOST are evaluated according to the classification rates by using the chi-square distance and the nearest neighborhood classifier. Moreover, the classic and latest texture classification methods, i.e., local binary pattern (LBP)[5] and its improved method LBP with variance (LBPV)[16] are adopted for comparison. For fair comparison, the size of the local region for all methods is set as 8-neighborhood.

The classification results on TC10 and TC12 are listed in Table 1. By comparing the proposed OST with the classic LBP, we can see that OST outperforms LBP on both TC10 and TC12, which achieves $20\% - 30\%$ increase on classification rates. Moreover, the proposed WOST performs a little worse than LBPV on TC10, but a little better than LBPV on TC12. In summary, the proposed WOST is comparable with the latest LBPV for texture classification.

The proposed OST/WOST is quite robust to disturb, while LBP/LBPV is too sensitive to small disturb. In order to give a clear view about the robustness, the effect of white noise on LBP/OST based histogram is analyzed. We only choose LBP/OST based textural histogram, rather than LBPV/WOST based histogram for this experiment. That is because the LBP/OST based textural histogram is directly calculated with the number of patterns, which can better represent the change on textural pattern.

Fig. 5 shows a texture image contaminated by two levels of noise, namely, weak white noise (with PSNR=30) and strong white noise (with PSNR=23) respectively. As shown in Fig. 5 (b), though it is contaminated by white noise, it is too weak to be sensed by the HVS. In other words, the HVS can hardly sense the noise in Fig. 5 (b), and the noise in it has limited damage on its textural information. The LBP is quite sensitive to any disturbance. As the blue and green bars shown in Fig. 6 (a), the LBP histograms of the original image (i.e., Fig. 5 (a)) and the weak noise contaminated image (i.e., Fig. 5 (b)) are quite different, which means the small disturbance changes the LBP histogram greatly. On the contrary, the weak noise has limited affection on the proposed OST based structure descriptor. As the blue and green bars shown in Fig. 6 (b), the two OST histograms for the original image and the weak noise contaminated image are quite similar. When the white noise becomes strong, the

Table 1: Texture classification rates (%) by different descriptors.

Algo. / DB.	LBP[5]	OST	LBPV[16]	WOST
TC10	55.16	84.53	**91.41**	88.83
TC12	49.00	71.81	76.41	**78.80**

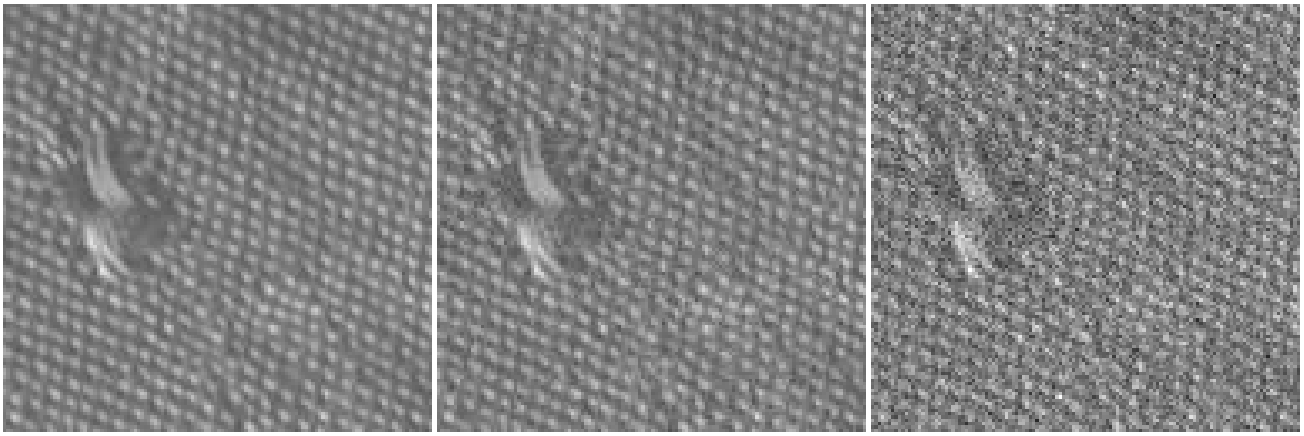

(a) Original Image (b) PSNR=30 (c) PSNR=23

Figure 5: Texture image distorted by different levels of white noise.

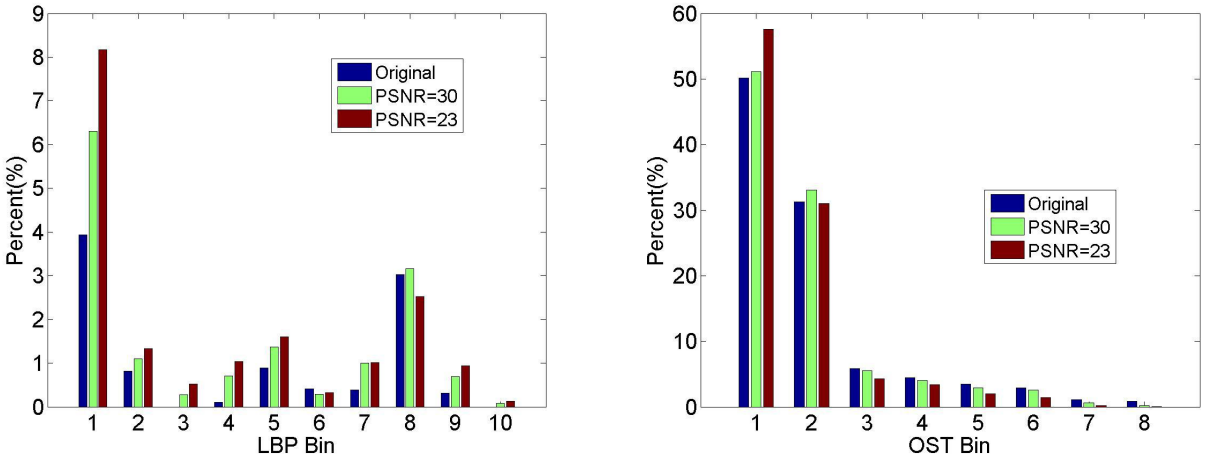

(a) LBP histogram (b) OST histogram

Figure 6: The robustness of the LBP/OST based structural histograms on noise.

Table 2: Classification rate (%) on contaminated images by different structure descriptors.

DB. \ Algo.	PSNR	LBP^5	OST	$LBPV^{16}$	WOST
TC10	30	44.19	80.78	86.88	**88.73**
	27	37.68	73.20	79.84	**87.27**
	23	24.74	61.59	62.27	**77.16**
TC12	30	44.61	69.49	73.84	**78.73**
	27	38.59	66.27	67.64	**77.64**
	23	26.81	52.73	53.84	**68.94**

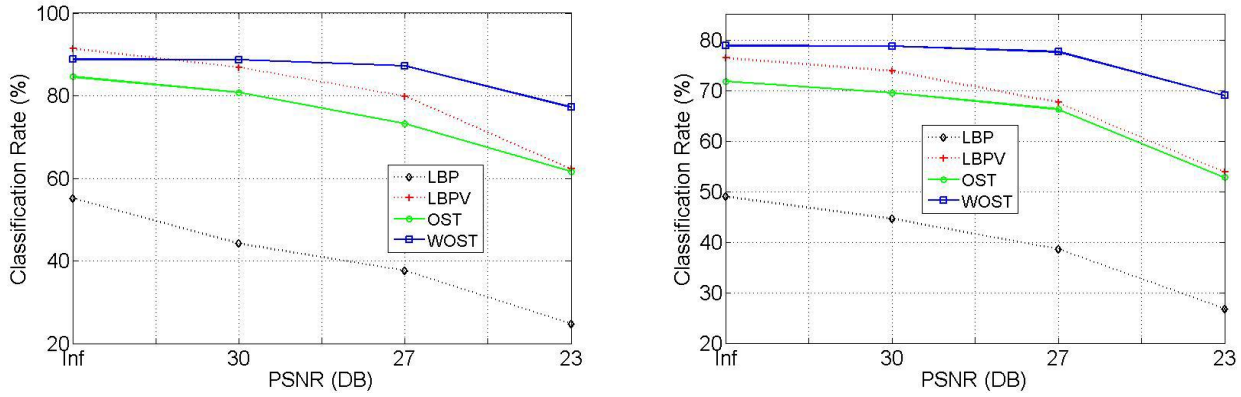

(a) TC10 (b) TC12

Figure 7: Decrease of classification rates under different levels of white noise.

visual content of Fig. 5 (c) is obviously distorted. Under the affection of strong white noise, both of the LBP and OST based histograms are obviously changed, as the red bars shown in Fig. 6 (a) and (b). According to the analysis above, we can conclude that the proposed OST based structure descriptor is robust to disturbance, and it performs quite consistently with the HVS.

In order to present a comprehensive analysis on the robustness of the proposed method against noise, the texture classification experiments on white noise contaminated TC10 and TC12 datasets are demonstrated. Firstly, different levels of white noise are injected into the two datasets. In this experiment, we choose three different levels of white noise: 1) PSNR=30dB, under which the image is slightly distorted; 2) PSNR=27dB, under which the image is obviously distorted; and 3) PSNR=23dB, under which the image is severely distorted.

The texture classification results on TC10 and TC12 are listed in Table 2, and the decreases of the classification rates against the original results are shown in Fig. 7. As the black dash lines shown in Fig. 7 (a) and (b), LBP is severely affected by noise, and the classification rates are obviously decreased with the increase of white noise. By comparing the green dash lines with black dash lines, we can see that OST is more robust to noise than LBP. Moreover, as shown in Table 2, OST achieves about 40% increase on TC10 against LBP under white noise, and achieves about 25% increase on TC12.

WOST also outperforms LBPV for white noise contaminated texture classification. As shown in Fig 7, the classification rates are almost unchanged on both datasets under weak white noise (PSNR=30), while the performance of LBPV for this is obviously decreased. When the white noise becomes stronger (PSNR=27), the classification rates from WOST have quite small decreases (-1.56% on TC10 and -1.16% on TC12), while that from LBPV is greatly decreased (-11.57% on TC10 and -8.77% on TC12). For the largest white noise (PSNR=23), the performance of both WOST and LBPV are decreased a lot, but WOST still performs much better than LBPV for this condition (WOST achieves about 15% increase than LBPV).

According to the analysis above, we can conclude that the proposed orientation selectivity based structure descriptor performs highly consistent with the HVS, which is robust to noise and outperforms the state-of-the-art algorithms for texture classification.

4. CONCLUSION

In this paper, we have introduced a novel structure descriptor based on the orientation selectivity mechanism of the primary visual cortex. The HVS is highly adaptive to extract structure for scene understanding, and structure character is widely used in image processing tasks. However, existing structure descriptors mainly describe the intensity change, but ignore spatial distribution of texture. Inspired by the orientation selectivity mechanism in the primary visual cortex, we imitated the excitatory/inhibitory interactions among nearby neurons and introduced an orientation selectivity based pattern to represent the spatial distribution of structure. Then, by combining the intensity change and the orientation selectivity based pattern, a novel structure descriptor was proposed. Experimental results on texture classification demonstrated that the proposed structure descriptor performs highly consistent with the HVS, which is rotation invariant and robust to disturbance.

ACKNOWLEDGMENTS

This work is supported by the Major State Basic Research Development Program of China (973 Program, No.2013CB329402), the NSF of China (Nos. 61401325 and 61401333), the Research Fund for the Doctoral Program of Higher Education (No. 20130203130001 and 20130203120009), and the Fundamental Research Funds for The Central Universities (No. JB140227 and K5051302096).

REFERENCES

1. D. Marr, "Visual information processing: the structure and creation of visual representations," *Philosophical transactions of the Royal Society of London. Series B, Biological sciences* **290**, pp. 199–218, 1980.
2. Z. Wang, A. C. Bovik, H. R. Sheikh, and E. P. Simoncelli, "Image quality assessment: from error visibility to structural similarity," *IEEE Transactions on Image Processing* **13**(4), pp. 600–612, 2004.
3. W. Lin and C. C. J. Kuo, "Perceptual visual quality metrics: A survey," *Journal of Visual Communication and Image Representation* **22**(4), pp. 297–312, 2011.
4. Y. Rui, T. S. Huang, and S. F. Chang, "Image retrieval: Current techniques, promising directions, and open issues," *Journal of Visual Communication and Image Representation* **10**(1), pp. 39–62, 1999.
5. T. Ojala, M. Pietikainen, and T. Maenpaa, "Multiresolution gray-scale and rotation invariant texture classification with local binary patterns," *IEEE Transactions on Pattern Analysis and Machine Intelligence* **24**(7), pp. 971–987, 2002.
6. A. Liu, W. Lin, and M. Narwaria, "Image quality assessment base on gradient similarity," *IEEE Transactions on Image Processing* **21**(4), pp. 1500–1512, 2012.
7. J. Wu, F. Qi, G. Shi, and Y. Lu, "Non-local spatial redundancy reduction for bottom-up saliency estimation," *Journal of Visual Communication and Image Representation* **23**(7), pp. 1158–1166, 2012.
8. J. Wu, W. Lin, and G. Shi, "Image quality assessment with degradation on spatial structure," *IEEE Signal Processing Letters* **21**(4), pp. 437–440, 2014.
9. T. Ojala, M. Pietikinen, and D. Harwood, "A comparative study of texture measures with classification based on featured distributions," *Pattern Recognition* **29**(1), pp. 51–59, 1996.
10. D. G. Lowe, "Distinctive image features from scale-invariant keypoints," *International Journal of Computer Vision* **60**(2), pp. 91–110, 2004.
11. D. H. Hubel and T. N. Wiesel, "Receptive fields and functional architecture in two nonstriate visual areas (18 and 19) of the cat," *Journal of neurophysiology* **28**, pp. 229–289, 1965.
12. D. H. Hubel and T. N. Wiesel, "Receptive fields, binocular interaction and functional architecture in the cat's visual cortex," *The Journal of Physiology* **160**(1), pp. 106–154, 1962.
13. T. D. Albright, "Direction and orientation selectivity of neurons in visual area MT of the macaque," *Journal of neurophysiology* **52**(6), pp. 1106–1130, 1984.

14. E. L. Bienenstock, L. N. Cooper, and P. W. Munro, "Theory for the development of neuron selectivity: orientation specificity and binocular interaction in visual cortex," *The Journal of neuroscience: the official journal of the Society for Neuroscience* **2**(1), pp. 32–48, 1982.
15. N. J. Priebe and D. Ferster, "Inhibition, spike threshold, and stimulus selectivity in primary visual cortex," *Neuron* **57**(4), pp. 482–497, 2008.
16. Z. Guo, L. Zhang, and D. Zhang, "Rotation invariant texture classification using LBP variance (LBPV) with global matching," *Pattern Recognition* **43**(3), pp. 706–719, 2010.
17. R. Shapley, M. Hawken, and D. Xing, "The dynamics of visual responses in the primary visual cortex," *Progress in brain research* **165**, pp. 21–32, 2007.
18. D. Hansel and C. Vreeswijk, "The mechanism of orientation selectivity in primary visual cortex without a functional map," *The Journal of Neuroscience* **32**(12), pp. 4049–4064, 2012.
19. D. Ferster and K. D. Miller, "Neural mechanisms of orientation selectivity in the visual cortex," *Annual review of neuroscience* **23**, pp. 441–471, 2000.
20. J. A. Cardin, L. A. Palmer, and D. Contreras, "Stimulus feature selectivity in excitatory and inhibitory neurons in primary visual cortex," *The Journal of neuroscience : the official journal of the Society for Neuroscience* **27**(39), pp. 333–344, 2007.
21. T. W. Troyer, A. E. Krukowski, N. J. Priebe, and K. D. Miller, "Contrast-invariant orientation tuning in cat visual cortex: Thalamocortical input tuning and correlation-based intracortical connectivity," *The Journal of Neuroscience* **18**(15), pp. 5908–5927, 1998.
22. D. Ferster, "Spatially opponent excitation and inhibition in simple cells of the cat visual cortex," *The Journal of Neuroscience* **8**(4), pp. 1172–1180, 1988.
23. F. W. Campbell and J. J. Kulikowski, "Orientational selectivity of the human visual system," *The Journal of Physiology* **187**(2), pp. 437–445, 1966.
24. T. Ojala, T. Maenpaa, M. Pietikainen, J. Viertola, J. Kyllonen, and S. Huovinen, "Outex - new framework for empirical evaluation of texture analysis algorithms," in *16th International Conference on Pattern Recognition*, **1**, pp. 701–706, 2002.